Published in final edited form as:
Cancer Prev Res (Phila). 2011 August ; 4(8): 1198–1208. doi:10.1158/1940-6207.CAPR-11-0188.

Selective PGE_2 suppression impairs colon carcinogenesis and modifies local mucosal immunity

Masako Nakanishi[1], **Antoine Menoret**[2], **Takuji Tanaka**[3], **Shingo Miyamoto**[1], **David C. Montrose**[1], **Anthony T. Vella**[2], and **Daniel W. Rosenberg**[1]

[1]Center for Molecular Medicine, University of Connecticut Health Center, Farmington, CT, USA

[2]Department of Immunology, University of Connecticut Health Center, Farmington, CT, USA

[3]Tohkai Cytopathology Institute: Cancer Research and Prevention, Gifu, Japan

Abstract

Prostaglandin E_2 (PGE_2) is a bioactive lipid that mediates a wide range of physiological effects and plays a central role in inflammation and cancer. PGE_2 is generated from arachidonic acid by the sequential actions of the cyclooxygenases (COXs) and terminal synthases (PGES). Increased levels of COX-2, with a concomitant elevation of PGE_2, are often found in colorectal cancers (CRC), providing the rationale for the use of COX-2 inhibitors for chemoprevention. Despite their proven efficacy in cancer prevention, however, COX-2 inhibitors exhibit dose-dependent toxicities that are mediated in part by their non-specific reduction of essential prostanoids, thus limiting their chemopreventive benefit. To achieve enhanced specificity, recent efforts have been directed towards targeting the inducible terminal synthase in the production of PGE_2, microsomal PGES (mPGES-1). In the present study, we show that genetic deletion of *mPGES-1* affords significant protection against carcinogen-induced colon cancer. *mPGES-1* gene deletion results in an ~80% decrease in tumor multiplicity and up to a 90% reduction in tumor load in the distal colon of azoxymethane (AOM)-treated mice. Associated with the striking cancer suppression, we have identified a critical role for PGE_2 in the control of immunoregulatory cell expansion (FoxP3-positive regulatory T cells) within the colon-draining mesenteric lymph nodes, providing a potential mechanism by which suppression of PGE_2 may protect against CRC. These results provide new insights into how PGE_2 controls anti-tumor immunity.

Keywords

Colorectal cancer; microsomal prostaglandin synthase-1; prostaglandin E_2; mucosal ulcer; regulatory T cells

Introduction

Selective inhibition of PGE_2 synthesis *via* pharmacologic targeting of mPGES-1 may provide chemopreventive efficacy while limiting the toxicity that is often associated with long-term use of COX-2 inhibitors (1). mPGES-1 is an inducible terminal synthase with only moderate expression under normal physiological conditions (2). However, coordinated induction of mPGES-1 and COX-2 is often observed within a variety of cancer types (3). Our laboratory recently reported that genetic deletion of *mPGES-1* in *Apc* mutant mice

To whom correspondence should be addressed: Daniel W. Rosenberg, PhD. Center for Molecular Medicine University of Connecticut Health Center 263 Farmington Avenue Farmington, CT 06030-3101 Phone: 1-860-679-8704 Fax: 1-860-679-7639 Rosenberg@nso2.uchc.edu.

significantly suppressed intestinal tumorigenesis, a protective effect that occurred in the absence of significant metabolic shunting of the COX-2 product, PGH_2, to other prostaglandins (4).

Despite the profound suppression in tumor formation that was observed in this earlier study, the effect of *mPGES-1* deletion in the colon was less apparent due to the propensity of *Apc* mutant mice to develop tumors in the small intestine (5). To address the issue of tissue-specificity, we introduced the *mPGES-1* gene deletion onto strain A mice, a line that is highly sensitive to chemical-induced colon cancer (6–8). In the following study, we examined the impact of *mPGES-1* genetic status on colon carcinogenesis induced by azoxymethane (AOM), an organo-specific carcinogen that causes multiple adenomas in the distal colon (8). Genetic deletion of *mPGES-1* affords significant protection against AOM-induced colon cancer. Associated with the striking cancer protection, we identified a critical role for PGE_2 in the control of immuno-regulatory cell expansion (FoxP3-positive regulatory T cells) within the colon-draining mesenteric lymph nodes, providing a potential mechanism by which inhibition of mPGES-1 and inducible PGE_2 synthesis may protect against CRC.

Materials and Methods

Generation of *mPGES-1* deletion on A/J background

Male A/J mice were purchased from The Jackson Laboratory (Bar Harbor, ME) and crossed with female *mPGES-1* knockout (KO) mice (C57BL/6) (9). *mPGES-1* heterozygous mice were backcrossed onto A/J mice for 9 additional generations (N10). N10 heterozygous mice were intercrossed to generate A/J:*mPGES-1* KO mice. Genotyping was performed by tail biopsy. Mice were maintained in a temperature-controlled, light-cycled room and allowed free access to drinking water and standard diet (LM-485, Harlan Teklad, Madison, WI).

Azoxymethane (AOM) treatment

Six week-old wild-type (WT) and KO mice were injected (*i.p.*) with 10 mg/kg of AOM (Sigma-Aldrich, MO) or vehicle control (0.9% NaCl) once a week for a total of 6 weeks. Twenty weeks after the last injection, mice were sacrificed and blood, spleen, mesenteric lymph node and colon were harvested for further analysis. Colons were flushed immediately with ice-cold PBS and excised longitudinally. Specimens were fixed-flat in 10% neutral buffered formalin for 4 hours and stored in 70% ethanol. Animal experiments were conducted after approval by the Animal Care Committee (ACC/IACUS) at the University of Connecticut Health Center.

Quantification of lesions

Whole-mount colons were stained with 0.2% methylene blue and the number and size of ACF and tumors were scored under a dissecting microscope. Colon tumor load per mouse was determined using tumor diameter to calculate the spherical tumor volume ($V=\frac{4}{3}\pi r^3$). The amount of ulcerated tissue was determined as the percent across the entire length of colon (n=10 per group).

Immunohistochemistry

Colons were paraffin-embedded and sectioned at 5-μm thickness. Sections were treated with 1–3% hydrogen peroxide, blocked and incubated with anti-APC (1:800; Millipore, Temecula, CA), anti-PCNA (1:150; Novocastra Laboratories Ltd., Newcastle upon Tyne, UK), anti-PECAM1 (1:500; Santa Cruz Biotechnologies, Inc, Santa Cruz, CA), anti-β-

catenin (1:2000; Sigma-Aldrich), anti-cleaved caspase-3 (1:200; Cell Signaling Technology Inc., Beverly, MA), anti-cyclinD1 (1:20; Novus Biologicals, Littleton, CO), anti-mPGES-1 (1:5000; Abnova, Taipei City, Taiwan) and anti-Ki-67 (1:50; Dako North America, Inc., Carpinteria, CA). Sections were incubated with biotinylated-secondary antibody, followed by ABC reagent (Vector Laboratories Inc., Burlingame, CA). Signal was detected using DAB solution (Vector Laboratories). Tissues were counterstained with hematoxylin.

Immunofluorescence microscopy

Following antigen retrieval, sections were blocked and incubated with anti-mPGES-1 (1:5000; Abnova) and then incubated with secondary antibody conjugated with Cy5 (1:500; Millipore). Nuclei were stained with Sytox Orange (1:10,000; Invitrogen). Staining was visualized by confocal microscopy using a Zeiss LSM 510/Confocor II and images were analyzed by LSM image browser software.

Flow cytometry

RBC-depleted spleens and mesenteric lymph node cells were re-suspended with staining buffer (BSS, 3% FBS and 0.1% sodium azide), followed by blocking solution containing normal mouse serum, anti-Fc receptor supernatant from the 2.4 G2 hybridoma (10), and human gamma-globulin. Cells were incubated with labeled primary antibodies (CD4, CD8, CD11b, Gr-1; eBioscience, San Diego, CA; Ki-67; BD Biosciences, Franklin Lakes, NJ) and analyzed by flow cytometry as described before (11). Intracellular staining of FoxP3 was performed according to manufacturer's porotocol (eBioscience).

In vitro lymphocytes stimulation

Spleens and mesenteric lymph nodes were harvested from 20–25-week old untreated female A/J mice, and 1×10^6 cells were stimulated with PMA (50 ng/ml; Sigma) and ionomycin (1μg/ml; Sigma) for 4 hrs in the presence of Brefeldin A (10μg/ml; Sigma). Intracellular staining was performed for IL-10, IFN-γ and Foxp3 (eBioscience,) as described earlier (n=6 per group).

Histological evaluation

Colon histology was evaluated on Swiss-rolled H&E sections by a board-certified pathologist (T.T.). Colonic crypt dysplasia was diagnosed according to established criteria (12), and colon tumors were further diagnosed using histopathological descriptions (13).

PGE_2 and serum cytokine analyses

Serum was prepared from blood and samples were purified using a PGE_2 affinity column (Cayman Chemical, Ann Arbor, MI). PGE_2 concentrations were determined by ELISA (Cayman Chemical) (n=13 per group). Serum cytokine levels were determined using a Bio-Plex Pro™ Assay (Bio-Rad Laboratories, Inc., Hercules, CA) (n=5 per group).

Measurement of the proliferative zone

Quantification of the proliferative zone was assessed on PCNA-stained tissues, randomly selecting 25 crypts per mouse for analysis (n=5 per group). The ratio of positive cells to total cells within the crypt was calculated for each colon, and an average of the ratios were compared between WT and *mPGES-1* KO mice.

Statistical analyses

Statistical analyses of tumor size and multiplicity, as well as a comparison of PGE_2 levels and the frequency of immune cells using FACS analysis, were performed by Student's *t*-test. A *p*-value less than 0.05 was considered statistically significant.

Results

mPGES-1 deletion suppresses colon carcinogenesis

mPGES-1 KO mice and WT littermates were injected with AOM and colons were harvested for analysis 20 weeks after the last injection. In response to AOM treatment, WT mice developed multiple, large and highly vascularized tumors, primarily confined to the distal colon (Fig. 1A: **arrows**). In *mPGES-1* KO mice, however, only several colons had macroscopically visible tumors (Fig. 1A). Tumor enumeration revealed a remarkable suppression (up to 85%) in *mPGES-1* KO mice (33.6 ± 2.0 versus 5.0 ± 0.7 in WT and KO, respectively; $P < 0.0001$; Fig. 1B), while tumor load was reduced by up to 90% (264.0 ± 29.0 versus 24.3 ± 4.3 in WT and KO, respectively; $P < 0.0001$; Fig. 1C). Despite the virtually complete protection against tumor formation, the total number of aberrant crypt foci (ACF), a pre-neoplastic lesion common to the distal colon, was reduced by less than 40% (32.4 ± 2.5 versus 20.7 ± 2.3 in WT and KO, respectively; $P < 0.002$; Fig. 1D). The most effective protection occurred in ACF of intermediate size, including those with 2–3 (16.0 ± 1.4 versus 10.0 ± 1.4 in WT and KO, respectively; $P < 0.005$) and 4–6 crypts per foci (10.4 ± 1.3 versus 6.3 ± 0.9 in WT and KO, respectively; $P < 0.01$).

In WT mice, analysis of tumor histology identified primarily two forms of large adenomas, characterized by either a pedunculated or flat morphology (Fig. 2A: **WT**). The tubular adenomas often exhibited an elongated structure with a stalk (Fig. 2A: **arrow**). In the *mPGES-1* KO mice, however, only 1 out of 19 mice developed a large adenoma (> 3 mm), which had either a flat or a slightly raised morphology (Fig. 2A: **KO**). Microadenomas were found in the colons from either genotype, although carcinomas *in situ* were limited to the WT mice (Fig. 2A). The microadenomas showed slight, moderate or severe nuclear atypia without evidence of expansion and invasive growth, characteristic of AOM-induced tumors occurring in this model (7, 12) (Fig. 2A). The morphology of the adenomas was similar between genotypes, comprised largely of microscopically tubular structures. However, tumors in WT mice were considerably larger, with frequent compression of surrounding normal crypts. In several cases, there was evidence for moderately differentiated tubular carcinomas *in situ* with invasive growth (Fig. 2A). Analysis of crypt dynamics revealed that within the normal colonic epithelium, the absence of *mPGES-1* did not affect overall crypt length nor alter the size of the proliferative compartment in comparison to the WT colons (Supplementary Fig. S1).

mPGES-1 status does not affect tumor markers

The profound suppression in tumor growth observed in the *mPGES-1* KO mice raised the possibility that PGE_2 levels may directly affect cell turnover within the tumor epithelium. To evaluate this possibility, colon tumors were examined immunohistochemically for PCNA staining (proliferation), and cleaved caspase-3, which detects an earlier stage of apoptosis in cells that have not yet undergone major morphological changes (14). A total of 10 colons from each genotype were selected for IHC analyses. Representative adenomas from a WT and *mPGES-1* KO colon are shown in Figure 3A. Intense PCNA staining was present throughout the tumor epithelium, regardless of *mPGES-1* genotype and independent of tumor size (Fig. 3A: **PCNA**). Cleaved caspase-3 immunostaining revealed few apoptotic cells within the normal crypts (data not shown), and their frequency was unaffected by *mPGES-1* status, nor affected by tumor size (Fig. 3A: **Cleaved caspase-3**). These

observations suggest that *mPGES-1* status does not influence cell turnover in the AOM colon tumor model.

In contrast to our previous findings, whereby deletion of *mPGES-1* was found to disrupt neovessel growth within small intestinal tumors in $Apc^{\Delta 14/+}$ mice (4), *mPGES-1* deletion did not directly affect PECAM-1 staining within and adjacent to AOM-induced colon tumors (Fig. 3A: **PECAM-1**). Even in the smallest colon lesions examined in the *mPGES-1* KO mice, PECAM-1 staining within the tumor stroma and surrounding colonic mucosa showed the presence of well-formed vascular structures (arrows) (Fig. 3A: **PECAM-1**). The difference in PECAM-1 staining between these two studies, however, may result from the dissimilar experimental systems employed, including differing genetic backgrounds and distinct mechanisms of tumor initiation.

We next examined the possibility that disruption of PGE_2 formation may directly impact Wnt signaling, an effect that was shown earlier in APC-deficient DLD-1 colon cancer cells (15). Surprisingly, loss of APC protein, with increased cytoplasmic staining and nuclear localization of β-catenin, was equivalent within tumors regardless of *mPGES-1* genotype or tumor size (Fig. 3B). The loss of APC protein is consistent with previous findings demonstrating that AOM-induced tumors do not express the full-length protein (16, 17). Taken together, these data suggest that the cancer suppression associated with reduced PGE_2 formation is not related to aberrant cell turnover or dysregulated β-catenin signaling in transformed epithelial cells.

mPGES-1 is expressed in the stroma in the colon

To define the localization of mPGES-1, immunofluorescence imaging was performed on colonic mucosa prepared from mice harboring tumors. In the WT colons, we identified increased expression of mPGES-1 localized primarily at the apical surface of the tumor stroma (Fig. 4). Positive staining was also found within the stroma immediately adjacent to the tumors (18) (Fig. 4: **arrows**). Similar to that reported by Murakami et al. (19), mPGES-1 staining was confined to the perinuclear region of the cells (Fig. 4). In addition, the expression of mPGES-1 was observed within multiple cell types, including macrophages and fibroblasts (20) (Supplementary Fig. S2). The location of mPGES-1 indicates that the primary source of inducible PGE_2 originates within the tumor stroma (21). Therefore, an alternative possibility for tumor suppression is that genetic deletion of *mPGES-1* interrupts localized production of PGE_2 within the tumor stroma, eliciting effects that extend into the epithelial compartment.

The presence of mucosal ulcerations in *mPGES-1* KO mice

Further evaluation of colon histology in the *mPGES-1* KO mice revealed the presence of synchronous, localized mucosal ulcerations affecting up to 15% of the colonic epithelium. These cryptal lesions developed independently of AOM treatment and were characterized histologically by the presence of regenerative atypia (Fig. 5A). Mucosal ulcerations within crypt abscesses resembled the active phase of ulcerative colitis. Regenerative crypts adjacent to the ulcerated areas, as well as infiltrating immune cells, were positive for Ki-67, indicating active cell proliferation (Fig. 5A: **Ki-67**). However, these regenerative crypts did not share other molecular features typically associated with neoplasia. For example, APC expression was largely retained compared to the extensive loss of APC protein observed in dysplastic adenomatous crypts in the *mPGES-1* KO mice (Fig. 5B: **APC**). Importantly, we found no evidence for β-catenin activation within these regenerative crypt lesions, with plasma membrane staining observed in all cases examined (Fig. 5B: β-**catenin**). Although cyclin D1, a key β-catenin target, showed intermittent nuclear staining within these

epithelial structures (Fig. 5B: **CyclinD1**), the normal status of APC expression and β-catenin localization within these colonic structures support their non-neoplastic nature.

Reduced frequency of CD4+FoxP3+ regulatory T cells in the draining mesenteric lymph nodes of the *mPGES-1*-null mice

The mild and localized chronic inflammation observed within the colons of *mPGES-1* KO mice was further substantiated by the presence of macroscopically inflamed mesenteric lymph nodes (MLN), with a significant expansion of total lymphocytes (1.6 ± 0.3 versus 7.4 ± 1.5 in WT and KO, respectively; $P < 0.006$; Fig. 6A). Total numbers of CD4+ and CD8+ cells were also markedly elevated (0.9 ± 0.2 versus 2.9 ± 0.5 for CD4+ in WT and KO, respectively; $P < 0.004$, 0.2 ± 0.04 versus 0.8 ± 0.2 for CD8+ in WT and KO, respectively; $P < 0.01$, respectively; Fig. 6A), presumably a direct result of the ongoing localized inflammation. In the spleen, however, there were no significant differences in the total numbers of both CD4+ and CD8+ cells (Fig. 6A). Correspondingly, serum PGE_2 concentrations were moderately ($p < 0.05$) lower in the *mPGES-1* KO compared to WT mice (Supplementary Fig. S3A). Moreover, the concentration of a panel of pro- and anti-inflammatory cytokines in the serum was mostly unchanged between genotypes, confirming the localized effect associated with *mPGES-1* deletion (Supplementary Fig. S3B). The only exception was a significant decrease in IL-1α in *mPGES-1* KO mice, which was recently demonstrated to be regulated by PGE_2 (22), and might be indicative of a stronger chronic inflammatory response.

We next investigated the immunoregulatory mechanisms that may underlie colonic inflammation in the *mPGES-1* KO mice. PGE_2 has been shown *in vitro* to enhance the differentiation of naive CD4+ T cells into FoxP3-positive regulatory T cells (T_{regs}) that have the potential to suppress effector T cell function (23). Furthermore, T_{regs} play an important regulatory role in gastrointestinal immunity (24). As shown in Figure 6B, in the MLN of *mPGES-1* KO mice, the frequency of CD4 FoxP3-double positive cells was reduced by 55% compared to WT mice (21.1 ± 1.1 versus 11.7 ± 1.3 in WT and KO, respectively; $P < 0.0004$). Importantly, this effect was not systemic, as the composition of T_{regs} within the spleen was unaffected by genotype (Fig. 6B).

We also examined the possibility that a population of myeloid-derived suppressor cells (MDSCs), immunomodulatory cells that are often increased in tumor-bearing mice (25), may be expanded in *mPGES-1* KO mice in response to the localized mucosal ulcerations. As anticipated, increased levels of GR-1 CD11b-double positive MDSCs were found in the MLN (0.03 ± 0.02 versus 0.20 ± 0.03 in WT and KO, respectively; $P < 0.00004$) and spleen (2.08 ± 0.40 versus 8.37 ± 2.76 in WT and KO, respectively; $P < 0.01$; Fig. 6C). However, the frequency of MDSCs was modest in comparison to changes found in other mouse tumor models. For example, in some cases the spleen can harbor up to 40% of MDSCs within the T cell population, depending of course on the underlying pathology (26). The present findings suggest that limited expansion of MDSCs in *mPGES-1* KO mice, most likely attributed to reduced PGE_2 levels (27), contributes to the enhanced inflammatory state that is present within the colon and that may ultimately impede colon tumor progression.

Based on the reduced levels of T_{regs} and the moderate effect on MDSCs, we postulated that additional immunoregulatory mechanisms might also contribute to tumor suppression. Thus to evaluate this possibility, we harvested cells from the spleens and MLNs of untreated WT and *mPGES-1* KO mice. The total number of cells harvested from the MLN of the *mPGES-1* KO mice was significantly higher in comparison to the WT mice, a result of the localized colonic ulcerations (Supplementary Fig. S4). In addition, the number of CD4+ and CD8+ cells were also markedly higher in the *mPGES-1* KO MLN (Supplemental Fig. S4), consistent with our findings in tumor bearing mice (Fig. 6A). Following a 4-hour stimulation

with PMA/ionomycin, the ability of CD4+ cells to produce IL-10 or IFN-γ was slightly impaired in the *mPGES-1* KO group (Supplemental Fig. S4). These observations suggest that *mPGES-1* deficiency may affect the production of T regulatory type 1 cells (Tr1), another type of immunoregulatory cell present within the gut mucosa (28).

Discussion

Elevated prostanoid production in the colon plays a key role in cancer pathogenesis and efforts have been made to suppress this pathway, primarily *via* inhibition of COX-2 activity. Although long-term COX-2 inhibition can be effective, it has also been associated with a number of adverse effects, notably cardiovascular and GI toxicities (29). Evidence from several tumor models provides the rationale for the development of alternative chemoprevention targets within the arachidonic acid pathway, including the terminal PGE_2 synthase, mPGES-1 (3). In the present study, we provide evidence that suppression of inducible PGE_2 production through genetic deletion of *mPGES-1* effectively reduces colon cancer development. We also go on to show that suppressing inducible PGE_2 formation influences cancer development in part by promoting an effective immune response to the tumor.

Remarkably, tumor suppression was so effective that only 1 out of 19 *mPGES-1* KO mice (5.3%) developed a colon tumor exceeding 3 mm in size. Despite this protection afforded to the colon, however, *mPGES-1* deletion did not influence the frequency of ACF to the same extent. This latter observation is consistent with the recent findings of Cho *et al*. (30) who reported that within a subset of patients on the Adenoma Prevention with Celecoxib) (APC)-trial, adenoma suppression by celecoxib treatment was not correlated with changes in the density of ACF within the distal colorectum. It is possible that at least for agents that target the COX-2 pathway, ACF do not provide a surrogate marker for colon cancer suppression.

PGE_2 is a pleiotropic molecule that is formed within a variety of cell types and can elicit effects that are both cell and tissue-context dependent. The precise location of inducible PGE_2 formation, however, remains somewhat controversial. For example, it is broadly accepted that tumor cell-derived PGE_2 promotes tumor growth through an autocrine mechanism. Consistent with this mechanism, mPGES-1 expression has been identified directly within the epithelial cells of colon tumors (31–33). In the present study, however, we found that mPGES-1 was localized primarily within the tumor stroma, indicating that inducible formation of PGE_2 may impair tumor expansion *via* non-cell autonomous mechanisms. This finding is consistent with the results of Kamei *et al*. (32), who showed that the growth of LLC lung tumor cells explanted into an *mPGES-1* deficient host was markedly impaired in comparison to the growth observed in an *mPGES-1* competent host. In addition, a number of studies have found COX-2 expression to be confined to the tumor stroma (Reviewed in 34).

The depletion of inducible PGE_2 formation is associated with the development of colonic mucosal abnormalities that are reminiscent of ulcerative colitis. The lesions are restricted to the large intestine. The histological features of these lesions consist of crypt erosion and an influx of inflammatory cells. Interestingly, Hara *et al*. (35) recently reported that *mPGES-1* KO mice demonstrate enhanced susceptibility to dextran sodium sulfate (DSS)-induced ulcerative colitis, confirming a critical role for PGE_2 in maintaining colonic epithelial barrier function under conditions of chemical-induced stress. It is possible that the localized ulcerations present within the colons of the *mPGES-1* KO mice induce a chronic inflammatory condition. We further speculate that this underlying inflammation may actually be a contributing factor in the suppression of colon tumors observed in the present study.

PGE_2 is among the most potent immuno-regulatory molecules active within the intestinal mucosa. In addition to its modulating effects on normal gut barrier function and mucosal response to pathogens (36), inducible formation of PGE_2 also plays a critical role in the immunosuppression associated with advanced neoplasia (37). Regulatory T cells (T_{regs}), with the potential to suppress effector T cell function (38, 39) have been shown to play an important immuno-modulatory role within the GI tract (24, 40). Within the tumor microenvironment, PGE_2 has been reported to enhance T_{reg} differentiation by inducing the expression of Foxp3 in naïve CD4+ T cells (23, 41, 42). In CRC patients, increased levels of T_{regs} were identified within the tumors as well as in the regional lymph nodes (43). Moreover, the effect of T_{regs} on the production of pro-inflammatory cytokines was reversed by treatment with non-steroidal anti-inflammatory drugs (NSAIDs), further evidence for T_{reg} dependence on PGE_2 during tumor evolution (43). Given the direct influence that PGE_2 elicits on FoxP3 expression in T cells, it is entirely possible that *mPGES-1* deficiency may result in a persistent over-reactive immune response due to the loss of functional activation of T_{regs}.

Interestingly, the present study shows that the impaired immuno-regulatory response in the *mPGES-1* KO mice, reflected by the spontaneous development of localized ulcerations, was not entirely accounted for by attenuated T_{reg} expansion. *mPGES-1* deletion also modestly affected the levels of MDSCs and Tr1-like cells, suggesting that the absence of inducible PGE_2 formation may disrupt fundamental immuno-modulatory mechanisms within the tumor microenvironment. One possibility is that *mPGES-1* deficiency causes a shift in cytokine profiles during tumorigenesis. In fact, Monrad *et al*. (44) recently showed that *mPGES-1* deficient bone marrow-derived dendritic cells (BMDCs) had decreased production of IL-12 in response to LPS stimulation. Furthermore, our preliminary data demonstrate that MLN cells harvested from the *mPGES-1* KO mice produce higher levels of several cytokines when compared to similarly stimulated WT cells (data not shown). Since the *mPGES-1* genotype did not affect systemic cytokine profiles with the exception of IL-1α, a more detailed analysis of tissue-specific cytokine profiles is warranted.

A number of studies suggest that chronic inflammation may play an important role in the pathogenesis of up to 20% of human cancers (45). In particular, long-standing inflammatory bowel disease (IBD) is considered a significant risk factor for CRC (46). Although the present data appear to contradict these earlier observations, we postulate that the underlying inflammation present in *mPGES-1* KO mice, resulting from the mild and localized colonic ulceration, may actually confer protection against tumor progression by providing a mechanism for active clearance of cancer-initiating cells. Consistent with this hypothesis, an earlier study by Tanaka *et al*. (13) demonstrated that mice administered DSS *prior* to a single injection of AOM failed to develop colon tumors 20 weeks later. In the present study, *mPGES-1* KO mice did not exhibit clinical signs of severe ulcerative colitis, such as rectal bleeding and excessive weight loss (data not shown), despite the presence of these benign, localized mucosal ulcerations. Of course the possibility exists that the mild inflammation that is present within the colons of the *mPGES-1* KO mice may contribute to subsequent cancer risk. However, without additional genetic hits, these lesions may not have the capacity to progress to cancer (47). Therefore, additional studies to better define the mechanisms by which selective suppression of PGE_2 directly modulates anti-tumor immunity and contributes to colon cancer suppression are underway. These studies will ultimately enable the development of effective therapeutic strategies for targeting mPGES-1 for cancer prevention.

Supplementary Material

Refer to Web version on PubMed Central for supplementary material.

Acknowledgments

We thank Dr. Robert Clark in Department of Immunology at University of Connecticut Health Center for his advice on designing experiments for T_{reg} analyses.

Grant Support This work was supported by NIH grant CA-125691 and CA-114635 (DWR).

References

1. Radmark O, Samuelsson B. Microsomal prostaglandin E synthase-1 and 5-lipoxygenase: potential drug targets in cancer. J Intern Med. 268:5–14. [PubMed: 20497297]
2. Samuelsson B, Morgenstern R, Jakobsson PJ. Membrane prostaglandin E synthase-1: a novel therapeutic target. Pharmacol Rev. 2007; 59:207–24. [PubMed: 17878511]
3. Nakanishi M, Gokhale V, Meuillet EJ, Rosenberg DW. mPGES-1 as a target for cancer suppression: A comprehensive invited review “Phospholipase A2 and lipid mediators”. Biochimie. 2010; 92:660–4. [PubMed: 20159031]
4. Nakanishi M, Montrose DC, Clark P, et al. Genetic deletion of mPGES-1 suppresses intestinal tumorigenesis. Cancer Res. 2008; 68:3251–9. [PubMed: 18451151]
5. Moser AR, Luongo C, Gould KA, McNeley MK, Shoemaker AR, Dove WF. ApcMin: a mouse model for intestinal and mammary tumorigenesis. Eur J Cancer. 1995; 31A:1061–4. [PubMed: 7576992]
6. Nambiar PR, Nakanishi M, Gupta R, et al. Genetic signatures of high- and low-risk aberrant crypt foci in a mouse model of sporadic colon cancer. Cancer Res. 2004; 64:6394–401. [PubMed: 15374946]
7. Papanikolaou A, Wang QS, Papanikolaou D, Whiteley HE, Rosenberg DW. Sequential and morphological analyses of aberrant crypt foci formation in mice of differing susceptibility to azoxymethane-induced colon carcinogenesis. Carcinogenesis. 2000; 21:1567–72. [PubMed: 10910960]
8. Rosenberg DW, Giardina C, Tanaka T. Mouse models for the study of colon carcinogenesis. Carcinogenesis. 2009; 30:183–96. [PubMed: 19037092]
9. Uematsu S, Matsumoto M, Takeda K, Akira S. Lipopolysaccharide-dependent prostaglandin E(2) production is regulated by the glutathione-dependent prostaglandin E(2) synthase gene induced by the Toll-like receptor 4/MyD88/NF-IL6 pathway. J Immunol. 2002; 168:5811–6. [PubMed: 12023384]
10. Unkeless JC, Kaplan G, Plutner H, Cohn ZA. Fc-receptor variants of a mouse macrophage cell line. Proc Natl Acad Sci U S A. 1979; 76:1400–4. [PubMed: 286323]
11. Menoret A, Myers LM, Lee SJ, Mittler RS, Rossi RJ, Vella AT. TGFbeta protein processing and activity through TCR triggering of primary CD8+ T regulatory cells. J Immunol. 2006; 177:6091–7. [PubMed: 17056535]
12. Nambiar, PR.; Nakanishi, M.; Gupta, RA., et al. Digestive Disease Week. New Orleans: 2004. Molecular signatures of high and low risk aberrant crypt foci in a mouse model of sporadic colon cancer; p. 5012004
13. Tanaka T, Kohno H, Suzuki R, Yamada Y, Sugie S, Mori H. A novel inflammation-related mouse colon carcinogenesis model induced by azoxymethane and dextran sodium sulfate. Cancer Sci. 2003; 94:965–73. [PubMed: 14611673]
14. Greenspan EJ, Nichols FC, Rosenberg DW. Molecular alterations associated with sulindac-resistant colon tumors in ApcMin/+ mice. Cancer Prev Res (Phila). 3:1187–97. [PubMed: 20716632]
15. Castellone MD, Teramoto H, Williams BO, Druey KM, Gutkind JS. Prostaglandin E2 promotes colon cancer cell growth through a Gs-axin-beta-catenin signaling axis. Science. 2005; 310:1504–10. [PubMed: 16293724]
16. Guda K, Upender MB, Belinsky G, et al. Carcinogen-induced colon tumors in mice are chromosomally stable and are characterized by low-level microsatellite instability. Oncogene. 2004; 23:3813–21. [PubMed: 15021908]

17. Maltzman T, Whittington J, Driggers L, Stephens J, Ahnen D. AOM-induced mouse colon tumors do not express full-length APC protein. Carcinogenesis. 1997; 18:2435–9. [PubMed: 9450492]
18. Takeda H, Sonoshita M, Oshima H, et al. Cooperation of cyclooxygenase 1 and cyclooxygenase 2 in intestinal polyposis. Cancer Res. 2003; 63:4872–7. [PubMed: 12941808]
19. Murakami M, Naraba H, Tanioka T, et al. Regulation of prostaglandin E2 biosynthesis by inducible membrane-associated prostaglandin E2 synthase that acts in concert with cyclooxygenase-2. J Biol Chem. 2000; 275:32783–92. [PubMed: 10869354]
20. Gudis K, Tatsuguchi A, Wada K, et al. Microsomal prostaglandin E synthase (mPGES)-1, mPGES-2 and cytosolic PGES expression in human gastritis and gastric ulcer tissue. Lab Invest. 2005; 85:225–36. [PubMed: 15531909]
21. Backlund MG, Mann JR, Dubois RN. Mechanisms for the prevention of gastrointestinal cancer: the role of prostaglandin E2. Oncology. 2005; 69(Suppl 1):28–32. [PubMed: 16210874]
22. Shao J, Sheng H. Prostaglandin E2 induces the expression of IL-1alpha in colon cancer cells. J Immunol. 2007; 178:4097–103. [PubMed: 17371964]
23. Sharma S, Yang SC, Zhu L, et al. Tumor cyclooxygenase-2/prostaglandin E2-dependent promotion of FOXP3 expression and CD4+ CD25+ T regulatory cell activities in lung cancer. Cancer Res. 2005; 65:5211–20. [PubMed: 15958566]
24. Read S, Malmstrom V, Powrie F. Cytotoxic T lymphocyte-associated antigen 4 plays an essential role in the function of CD25(+)CD4(+) regulatory cells that control intestinal inflammation. J Exp Med. 2000; 192:295–302. [PubMed: 10899916]
25. Ostrand-Rosenberg S, Sinha P. Myeloid-derived suppressor cells: linking inflammation and cancer. J Immunol. 2009; 182:4499–506. [PubMed: 19342621]
26. Gabrilovich DI, Nagaraj S. Myeloid-derived suppressor cells as regulators of the immune system. Nat Rev Immunol. 2009; 9:162–74. [PubMed: 19197294]
27. Sinha P, Clements VK, Fulton AM, Ostrand-Rosenberg S. Prostaglandin E2 promotes tumor progression by inducing myeloid-derived suppressor cells. Cancer Res. 2007; 67:4507–13. [PubMed: 17483367]
28. Vieira PL, Christensen JR, Minaee S, et al. IL-10-secreting regulatory T cells do not express Foxp3 but have comparable regulatory function to naturally occurring CD4+CD25+ regulatory T cells. J Immunol. 2004; 172:5986–93. [PubMed: 15128781]
29. Wang D, Dubois RN. The role of COX-2 in intestinal inflammation and colorectal cancer. Oncogene. 29:781–8. [PubMed: 19946329]
30. Cho NL, Redston M, Zauber AG, et al. Aberrant crypt foci in the adenoma prevention with celecoxib trial. Cancer Prev Res (Phila). 2008; 1:21–31. [PubMed: 19138933]
31. Golijanin D, Tan JY, Kazior A, et al. Cyclooxygenase-2 and microsomal prostaglandin E synthase-1 are overexpressed in squamous cell carcinoma of the penis. Clin Cancer Res. 2004; 10:1024–31. [PubMed: 14871981]
32. Kamei D, Murakami M, Sasaki Y, et al. Microsomal prostaglandin E synthase-1 in both cancer cells and hosts contributes to tumour growth, invasion and metastasis. Biochem J. 2009
33. Yoshimatsu K, Golijanin D, Paty PB, et al. Inducible microsomal prostaglandin E synthase is overexpressed in colorectal adenomas and cancer. Clin Cancer Res. 2001; 7:3971–6. [PubMed: 11751489]
34. Williams CS, DuBois RN. Prostaglandin endoperoxide synthase: why two isoforms? Am J Physiol. 1996; 270:G393–400. [PubMed: 8638704]
35. Hara S, Kamei D, Sasaki Y, Tanemoto A, Nakatani Y, Murakami M. Prostaglandin E synthases: Understanding their pathophysiological roles through mouse genetic models. Biochimie. 2010; 92:651–9. [PubMed: 20159030]
36. Montrose DC, Kadaveru K, Ilsley JN, et al. cPLA2 is protective against COX inhibitor-induced intestinal damage. Toxicol Sci. 117:122–32. [PubMed: 20562220]
37. Tilley SL, Coffman TM, Koller BH. Mixed messages: modulation of inflammation and immune responses by prostaglandins and thromboxanes. J Clin Invest. 2001; 108:15–23. [PubMed: 11435451]
38. Sakaguchi S, Sakaguchi N, Asano M, Itoh M, Toda M. Immunologic self-tolerance maintained by activated T cells expressing IL-2 receptor alpha-chains (CD25). Breakdown of a single mechanism

of self-tolerance causes various autoimmune diseases. J Immunol. 1995; 155:1151–64. [PubMed: 7636184]

39. Seddon B, Mason D. Regulatory T cells in the control of autoimmunity: the essential role of transforming growth factor beta and interleukin 4 in the prevention of autoimmune thyroiditis in rats by peripheral CD4(+)CD45RC-cells and CD4(+)CD8(−) thymocytes. J Exp Med. 1999; 189:279–88. [PubMed: 9892610]
40. Maloy KJ, Salaun L, Cahill R, Dougan G, Saunders NJ, Powrie F. CD4+CD25+ T(R) cells suppress innate immune pathology through cytokine-dependent mechanisms. J Exp Med. 2003; 197:111–9. [PubMed: 12515818]
41. Mahic M, Yaqub S, Johansson CC, Tasken K, Aandahl EM. FOXP3+CD4+CD25+ adaptive regulatory T cells express cyclooxygenase-2 and suppress effector T cells by a prostaglandin E2-dependent mechanism. J Immunol. 2006; 177:246–54. [PubMed: 16785520]
42. Baratelli F, Lin Y, Zhu L, et al. Prostaglandin E2 induces FOXP3 gene expression and T regulatory cell function in human CD4+ T cells. J Immunol. 2005; 175:1483–90. [PubMed: 16034085]
43. Yaqub S, Henjum K, Mahic M, et al. Regulatory T cells in colorectal cancer patients suppress anti-tumor immune activity in a COX-2 dependent manner. Cancer Immunol Immunother. 2008; 57:813–21. [PubMed: 17962941]
44. Monrad SU, Kojima F, Kapoor M, et al. Genetic deletion of mPGES-1 abolishes PGE2 production in murine dendritic cells and alters the cytokine profile, but does not affect maturation or migration. Prostaglandins Leukot Essent Fatty Acids. 84:113–21. [PubMed: 21190819]
45. Aggarwal BB, Vijayalekshmi RV, Sung B. Targeting inflammatory pathways for prevention and therapy of cancer: short-term friend, long-term foe. Clin Cancer Res. 2009; 15:425–30. [PubMed: 19147746]
46. Waldner MJ, Neurath MF. Colitis-associated cancer: the role of T cells in tumor development. Semin Immunopathol. 2009; 31:249–56. [PubMed: 19495757]
47. Mladenova D, Daniel JJ, Dahlstrom JE, et al. The NSAID sulindac is chemopreventive in the mouse distal colon but carcinogenic in the proximal colon. Gut. 60:350–60. [PubMed: 20980345]

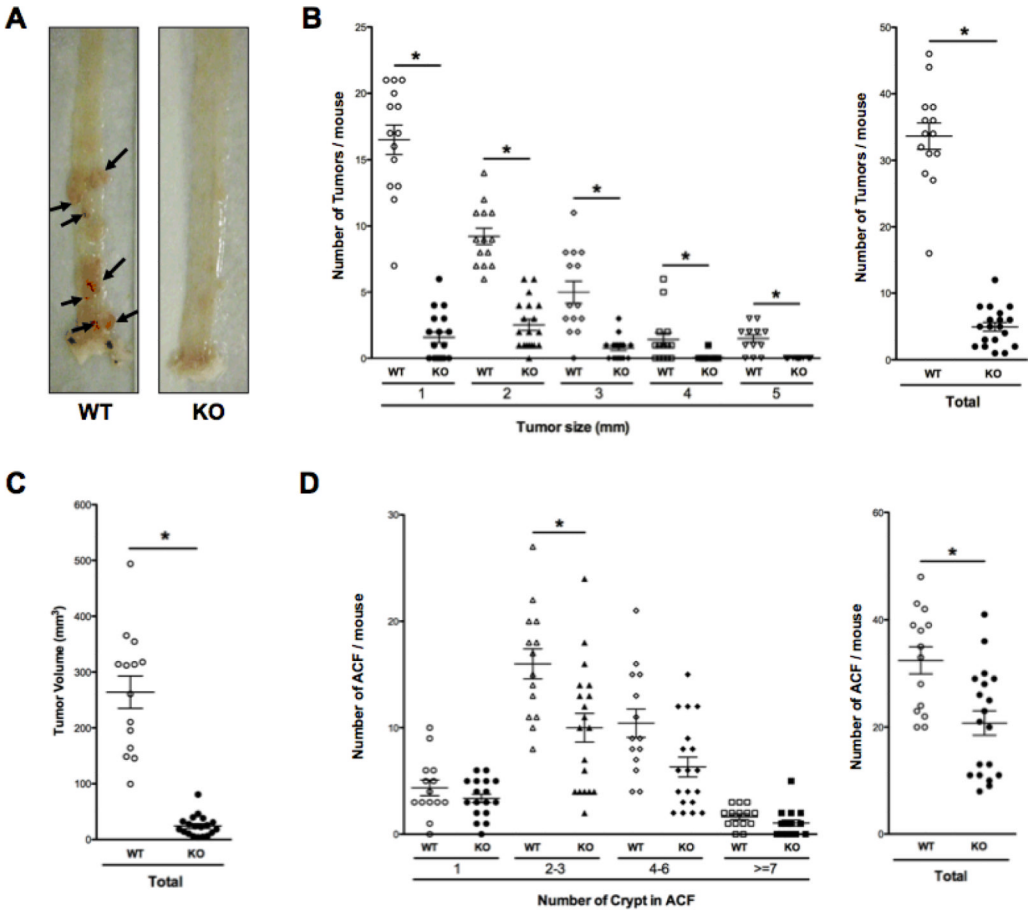

Figure 1. Genetic deletion of *mPGES-1* suppresses AOM-induced colon cancer

A, Representative whole-mount colons showing numerous large, well-vascularized tumors in the WT mice (arrows). B, Size distribution and total number of tumors per colon rounded to the nearest whole number, as well as total tumor volume (mm^3). C, Size distribution and total number of ACF. Each data point represents an individual mouse. Bars indicate means ± S.E.M. * $P < 0.05$ compared to WT mice.

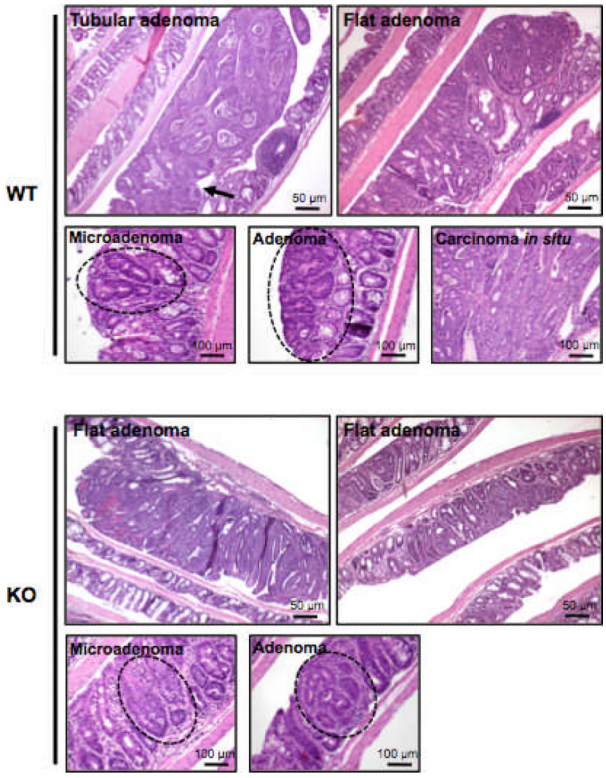

Figure 2. Evaluation of colonic lesions

Tumors in WT mice exhibit tubular or flat adenoma, while *mPGES-1* KO mice only develop flat or slightly raised adenomas. Microadenomas and adenomas were found in the colons of both genotypes. Carcinomas *in situ* were identified only in the WT colons. Lesions are delineated by a dotted line. $n = 14$ in WT and $n = 19$ in KO mice. Scale bars as indicated.

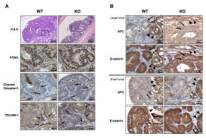

Figure 3. Immunohistochemical analysis of colon tumor markers

A, Representative serial sections of colons showing staining for PCNA, cleaved caspase-3, and PECAM-1, where positive staining is indicated by the arrows. Boxed areas in H & E sections were enlarged to show the positive staining. Scale bars as indicated. B, Representative images of large and small tumors from each genotype, stained for APC and β-catenin. Tumor cells from either genotype lack expression of APC (arrows) compared to adjacent normal crypts (arrow-heads), independent of tumor size. Similarly, β-catenin staining is increased in the tumor cells (arrows) compared to adjacent normal cells (arrow heads), independent of genotype or tumor size. n = 10 per group. Scale bars as indicated.

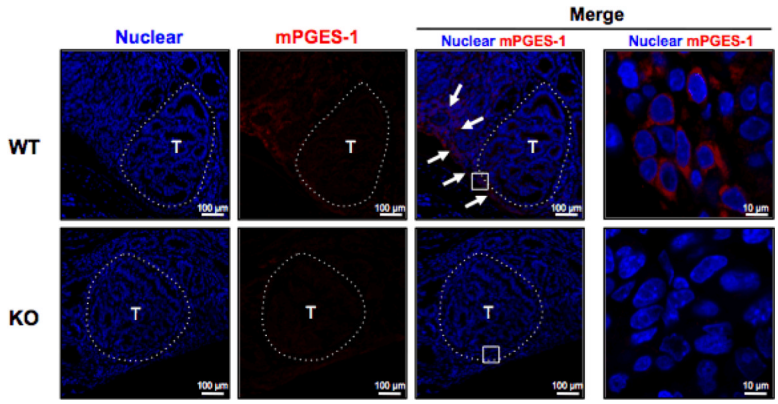

Figure 4. Immunolocalization of mPGES-1 in tumor stroma

Immunofluorescence detection of mPGES-1 in tumor and adjacent normal colonic mucosa after AOM exposure. T identifies tumor area (delineated by dotted line). Arrows in the merged images indicate the presence of mPGES-1-expressing cells at the apical surface of the tumor and also within the adjacent tumor stroma in WT mice. mPGES-1 was localized to the perinuclear region of stromal cells abutting the tumor. Scale bars as indicated.

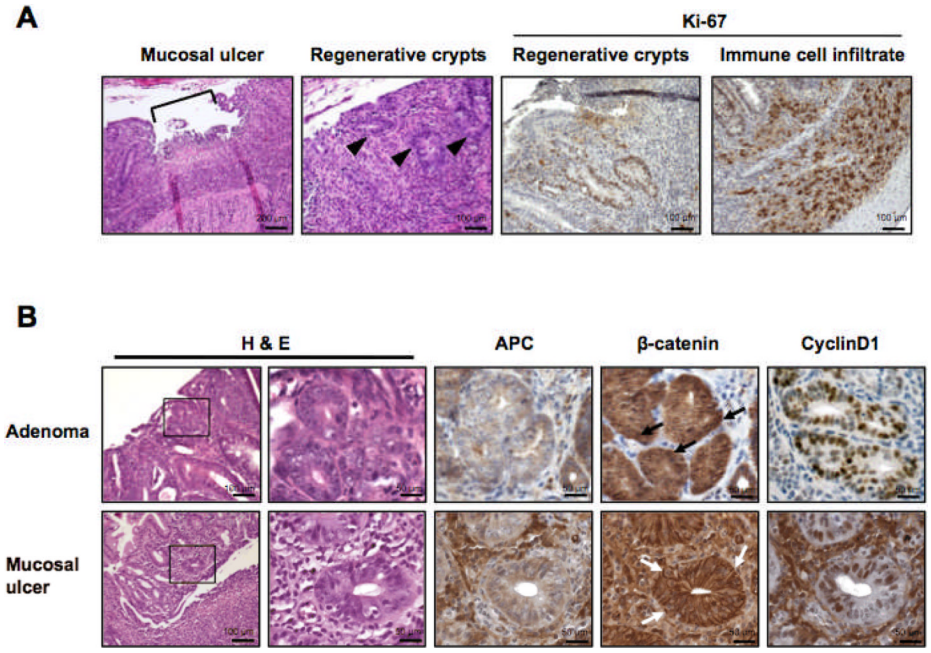

Figure 5. Histological features of localized colonic ulcerations

A, A representative localized ulceration in the colon of a *mPGES-1* KO mouse containing regenerative crypts (arrowheads). Highly proliferative cells within the regenerative crypts are detected by Ki-67 staining. Intense Ki-67 staining is also seen in infiltrating immune cells within the colonic mucosa. B, Comparison of tumor-related markers in serial sections of tumors and mucosal ulcers in *mPGES-1* KO mice. Enlarged areas are identified by the box. Scale bars as indicated.

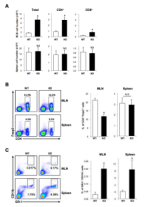

Figure 6. Flow cytometry of cells in mesenteric lymph nodes (MLN) and spleens

A, Total numbers of cells in MLN and spleen, including the relative frequency of $CD4^+$ and $CD8^+$ T cells. B, Representative FACS analysis showing the frequency of CD4 FoxP3 double positive T_{regs}. Quantification of FACS analyses is expressed as means ± S.E.M, n = 9 per group. C, Representative FACS analysis showing frequency of Gr-1 CD11b double positive MDSCs. Quantification of FACS analysis is expressed as means ± S.E.M, n = 8 in WT and n = 6 in KO mice. * $P < 0.05$; N.S., not significant compared to WT mice.